Journal of Alloys and Compounds 536S (2012) S190–S193

Contents lists available at SciVerse ScienceDirect

Journal of Alloys and Compounds

journal homepage: www.elsevier.com/locate/jallcom

Microstructure of low stacking fault energy silver processed by different routes of severe plastic deformation

Zoltán Hegedűs[a], Jenő Gubicza[a,*], Megumi Kawasaki[b], Nguyen Q. Chinh[a], Zsolt Fogarassy[c], Terence G. Langdon[b,d]

[a] Department of Materials Physics, Eötvös Loránd University, Pázmány Péter sétány. 1/A, H-1117 Budapest, Hungary
[b] Departments of Aerospace & Mechanical Engineering and Materials Science, University of Southern California, Los Angeles, CA 90089-1453, USA
[c] Research Institute for Technical Physics and Materials Science, P.O.Box 49, H-1525 Budapest, Hungary
[d] Materials Research Group, School of Engineering Sciences, University of Southampton, Southampton SO17 1BJ, UK

ARTICLE INFO

Article history:
Received 3 June 2011
Received in revised form 12 October 2011
Accepted 19 October 2011
Available online 7 November 2011

Keywords:
Silver
Stacking fault energy
Dislocations
Twins
Equal-channel angular pressing
High-pressure torsion

ABSTRACT

Samples of 4 N purity Ag were processed at room temperature (RT) by equal-channel angular pressing (ECAP) and high-pressure torsion (HPT) up to 8 passes and 20 revolutions, respectively. It was found that the minimum grain size was around 200 nm for both ECAP and HPT. However, the dislocation density and the twin boundary frequency were about three times larger in HPT due to the very high applied hydrostatic pressure. The maximum dislocation density (about 1.5×10^{16} m^{-2}) and twin boundary frequency (about 2%) achieved by HPT at RT are extremely high among pure fcc metals and this can be explained by the difficult annihilation of the highly dissociated dislocations due to the very low stacking fault energy in Ag.

1. Introduction

Contamination- and porosity-free bulk ultrafine-grained (UFG) metals and alloys can be processed by severe plastic deformation (SPD) [1,2]. The high pressure applied during these procedures enables the evolution of a high dislocation density in two ways: (i) by impeding the vacancy migration that hinders the annihilation of dislocations and (ii) by suppressing the cracking thereby keeping the integrity of the workpiece even at high strains. The high dislocation density and the fine-grained microstructure lead to high strength in these materials. Equal-channel angular pressing (ECAP) and high-pressure torsion (HPT) are the most studied SPD procedures in the literature [1,2]. The effect of high pressure on the formation of UFG microstructure can be evaluated by comparing materials processed by ECAP and HPT as the pressure applied in the latter procedure is usually one order of magnitude larger than in the former case. The evolutions of the microstructures during ECAP and HPT have been studied extensively for face-centered cubic (fcc) metals having medium or high stacking fault energies (SFEs) [2–8]. It was found that the minimum grain size achieved at room temperature (RT) was not greatly dependent on the method of processing. For instance, in the case of Cu deformed by ECAP the saturation grain size is about 200 nm and this is only slightly larger than the minimum grain size, 160 nm, obtained by HPT [9]. At the same time, the dislocation density is 2–3 times larger in the case of HPT as the higher pressure hinders the annihilation of dislocations [9]. However, to the knowledge of the authors, very little information is available on the microstructures developed during SPD in pure fcc metals having low SFE, such as Ag [10,11]. In a recently published report [12], the microstructural evolution in 4N5 purity Ag were studied as a function of the number of ECAP passes (the notation of 4 N purity was a misprint in that paper). Due to the low impurity content, the highly distorted HPT samples became self-annealed very quickly, even before it was possible to study their microstructures, and therefore a comparison between ECAP- and HPT-processed Ag samples required an increase in the impurity level. In the present study, the evolution of microstructures in 4 N purity Ag during ECAP and HPT are presented and the effect of pressure on the defect structure is discussed.

2. Experimental materials and procedures

99.99 at.% (4 N) purity Ag samples were manufactured by American Elements. Before SPD-processing the samples were annealed at 741 K for 1 h. This temperature

* Corresponding author. Tel.: +36 1 372 2876, fax: +36 1 372 2811.
E-mail address: gubicza@metal.elte.hu (J. Gubicza).

0925-8388/$ – see front matter © 2011 Elsevier B.V. All rights reserved.
doi:10.1016/j.jallcom.2011.10.070

corresponds to 0.6 T_m, where T_m is the absolute melting point of Ag. Annealed billets having lengths of approx. 70 mm and diameters of 10 mm were pressed through 1, 4 and 8 passes of ECAP at RT with a pressing velocity of 8 mm s^{-1}. The pressing was conducted using route B_c where the billet is rotated in the same sense by 90° about its longitudinal axis after each pass [13]. The die had an internal channel angle of 90° and an outer arc of curvature of 20°. In this configuration, one pass corresponds to an equivalent strain of ~1 [14].

Annealed disks having 10 mm diameter and 0.8 mm initial thickness were processed by HPT for 1, 10 and 20 revolutions at RT. The applied pressure and the speed of revolution were 6 GPa and 1 rpm, respectively. The equivalent strain in the HPT-processed disks is proportional to the number of revolutions and the distance from the center. For instance, after 1 revolution at the half-radius of the disk the equivalent strain is about 11.3 [2].

The grain structure was examined using a FEI Quanta 3D scanning electron microscope (SEM) and a Philips CM-20 transmission electron microscope (TEM) operating at 200 kV. The TEM samples were mechanically thinned to ~80 μm, cooled to liquid nitrogen temperature and then thinned with 6 keV Ar^+ ions from both sides until perforation. Finally, a thin damaged layer was removed using 2 keV Ar^+ ions. The lattice defects were examined by X-ray line profile analysis on the surface of HPT disks and on transverse sections cut perpendicular to the axes of the ECAP billets. The measurements of the X-ray diffraction lines were performed using a special high-resolution diffractometer (Nonius FR591) with CuKα_1 radiation (λ = 0.15406 nm). The line profiles were evaluated using the extended Convolutional Multiple Whole Profile (eCMWP) fitting procedure [15]. In this method, the diffraction pattern is fitted by the sum of a background spline and the convolution of the instrumental pattern and the theoretical line profiles related to the crystallite size, dislocations and twin faults. This method gives the crystallite size, the dislocation density and the twin boundary frequency with good statistics, where the twin boundary frequency is defined as the fraction of twin boundaries among the {1 1 1} lattice planes.

3. Results and discussion

The SEM image in Fig. 1a illustrates the grain structure in the annealed initial state. The mean grain size in the initial material was ~56 μm. After one pass of ECAP the mean grain size was reduced to 20 μm as shown in Fig. 1b. The TEM image in Fig. 2a shows that after 4 passes the grain size decreased to 230 nm and further ECAP deformation up to 8 passes gave no additional grain refinement. In our previous paper, the evolution of the microstructure in 4N5 purity Ag as a function of number of ECAP passes was presented [12]. The mean grain size in 4N5 purity Ag after 4 passes was also about 200 nm indicating that a two times larger impurity content in the present case did not affect significantly the minimum grain size achievable by ECAP.

The crystallite size for the 4 N purity samples processed by either ECAP or HPT was between 40–50 nm irrespective of the numbers of passes or revolutions, respectively, as determined by X-ray line profile analysis. It is noted that the crystallite size measured by line profile analysis is smaller than the grain size obtained by TEM and that is a common observation for bulk UFG metals processed by severe plastic deformation methods. This difference arises because the crystallites are equivalent to domains in the microstructure which scatter X-rays coherently. As the coherency of X-rays breaks even if they are scattered from volumes having quite small misorientations (1–2°), the crystallite size corresponds rather to the size of dislocation cells and/or subgrains in the severely deformed microstructures.

Fig. 3 shows the dislocation density and the twin boundary frequency in 4 N purity Ag as a function of the number of ECAP passes as determined by X-ray line profile analysis. The dislocation density increased up to 4 passes and thereafter it remained unchanged within the experimental error between 4 and 8 passes. The saturation value of the dislocation density is $46 \pm 5 \times 10^{14}$ m^{-2} and this value is very large compared with other pure fcc metals processed by ECAP. This large value can be attributed to the low SFE that results in a high degree of dislocation dissociation into partials. The large splitting distance between partials hinders the dislocation annihilation during SPD thereby leading to a high saturation dislocation density. The twin boundary frequency was 0.4 ± 0.1% after the first ECAP pass and reached a maximum value of 0.8 ± 0.1% after

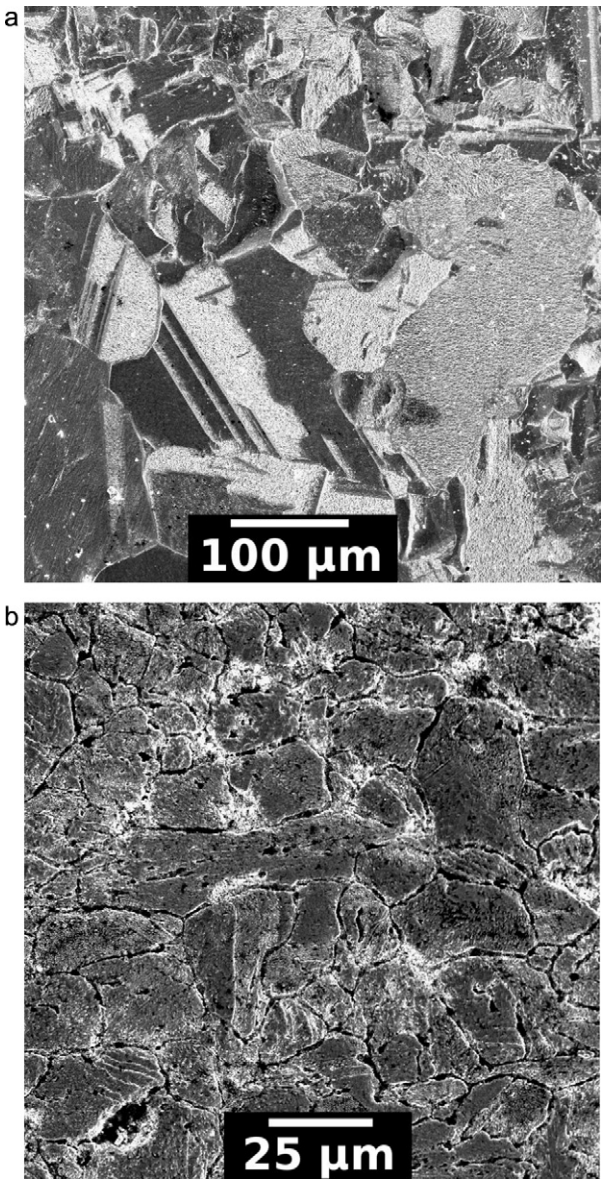

Fig. 1. SEM images taken on the annealed initial state (a) and after 1 pass of ECAP (b).

4 passes. Further processing up to 8 passes caused a slight decrease in the twin boundary frequency. It should be noted that the relative intensity of reflection 2 2 0 in the X-ray diffraction patterns for the ECAP-processed samples was higher than the value for a random crystallographic orientation. This indicates a weak texture with a preferred ⟨2 2 0⟩ crystallographic orientation in the direction of the longitudinal axis of the billet. However, this texture does not require any change in the evaluation method of the X-ray line profiles as the very large strain during severe plastic deformation guarantees the population of all the slip systems by dislocations that was assumed in the microstructural model of the present X-ray line profile analysis. In the case of HPT-processed samples, a texture was not observed.

The microstructures of the HPT-processed disks were investigated close to the center, at the half radius and the periphery by X-ray line profile analysis. The dislocation density and the twin boundary frequency are plotted in Fig. 4a as a function of the distance from the center of the disks. The dimensions of the area illuminated by X-rays were 0.3 and 1.5 mm parallel and perpendicular to the disk radius, respectively. This is reflected

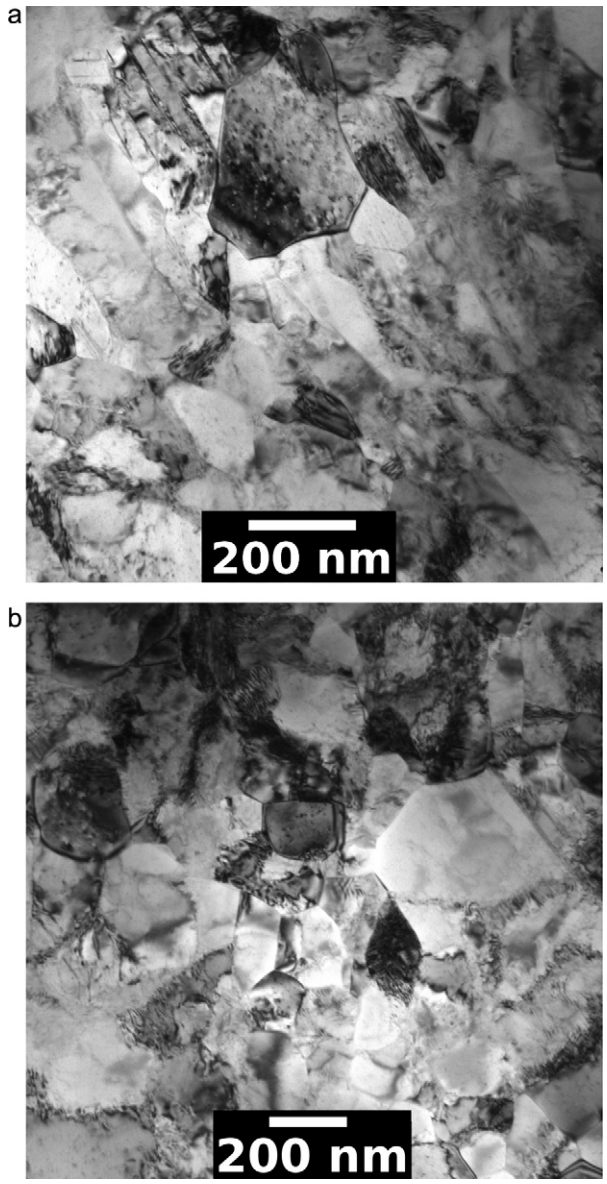

Fig. 2. TEM images of the microstructures after 4 ECAP passes (a) and 20 HPT revolutions (b).

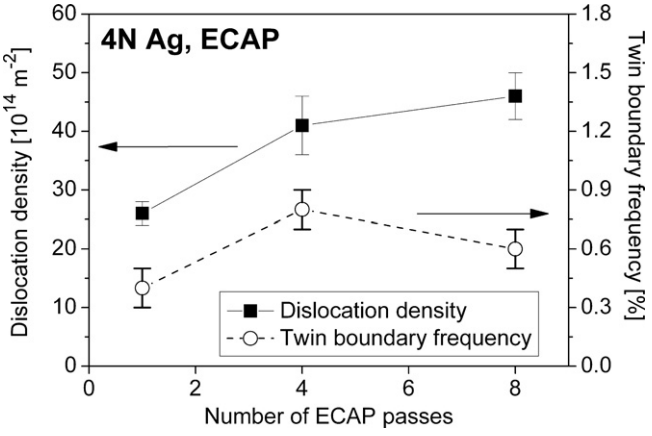

Fig. 3. The dislocation density and the twin boundary frequency as a function of number of ECAP passes.

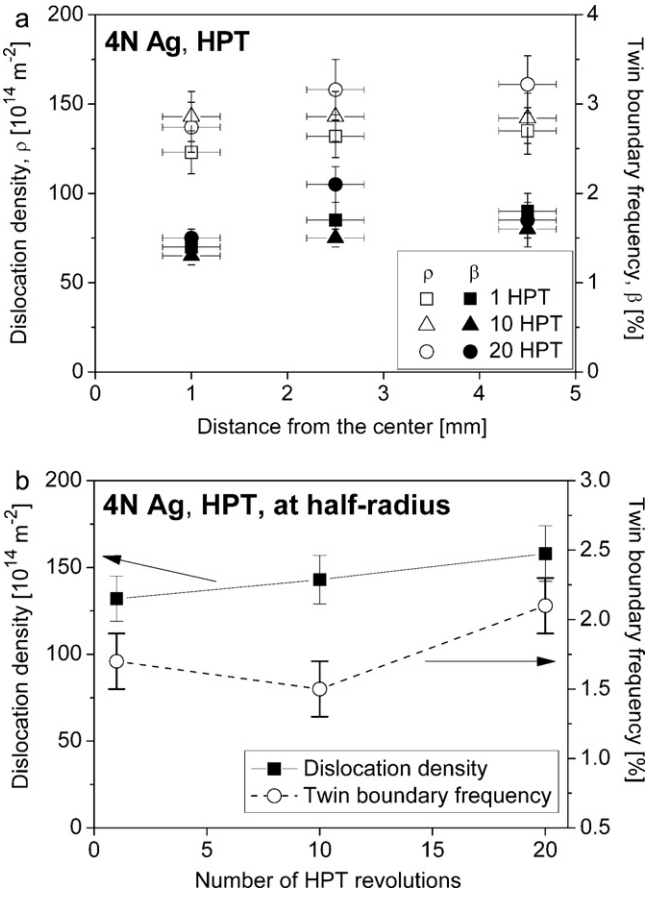

Fig. 4. The dislocation density and the twin boundary frequency as a function of the distance from the center in the HPT disks for different numbers of revolutions (a). The dislocation density and the twin boundary frequency measured at the half-radius of the disks as a function of number of HPT revolutions (b).

by the horizontal error bars of the datum points in Fig. 4a. It can be seen that the defect densities change only slightly along the radius of the HPT disks. Therefore, we take the values measured at the half-radius as representative for a certain number of revolutions and these values are plotted in Fig. 4b. The dislocation density and the twin boundary frequency reached very high values of $132 \pm 13 \times 10^{14}\,m^{-2}$ and $1.7 \pm 0.2\%$, respectively, even after 1 revolution and they increased only slightly during further HPT-processing. The maximum dislocation density and twin boundary frequency at the half radius of the HPT disks were $154 \pm 16 \times 10^{14}\,m^{-2}$ and $2.1 \pm 0.2\%$, respectively, reached after 20 revolutions. These defect densities are about three times larger than the saturation values for ECAP and they can be explained by the high applied pressure of $P = 6$ GPa. Previous reports [e.g. 16] have shown that in the case of ECAP the magnitude of pressure can be approximated by the flow stress (~300 MPa for Ag [12]) that is about one order of magnitude smaller than for HPT. The high pressure applied during HPT retards vacancy migration as the migration enthalpy is the sum of the migration energy ($E_{VM} = 0.66$ eV [17]) and PV where V is the volume of a vacancy ($9 \times 10^{-30}\,m^3$ in Ag calculated as the half of the volume per atom in the lattice). For HPT-processed Ag, PV = 0.34 eV resulting in a five orders of magnitude smaller diffusion coefficient than in the case of ECAP as determined by a comparison of the values of the term of $\exp[-(E_{VM} + PV)/kT]$ where k is the Boltzmann-constant and T is 300 K. This slower diffusion hinders the climb-controlled dislocation annihilation resulting in very large dislocation density. Previous investigations [9] on Cu having a medium SFE revealed

a similar ratio between the dislocations densities reached by HPT and ECAP. However, the twinning activity in Cu was not affected significantly by the pressure. The plastic deformation in low SFE Ag occurs by both dislocation slip and twinning. The twin faults usually form at glide obstacles, such as Lomer-Cottrell locks and grain boundaries where the local stress exceeds the critical stress required for twin nucleation. The number of these nucleation sites increases if the dislocation density is higher and this leads to a larger twin boundary frequency in the case of HPT compared with ECAP.

TEM investigations performed at the half radius of the HPT disks have shown that the grain structure is similar for the HPT-processed samples irrespective of the number of revolutions. Fig. 2b illustrates the microstructure after 20 revolutions. The mean grain size was 220 nm and that is very close to the saturation values determined for the ECAP-processed specimens. This indicates that the lattice defect densities are more sensitive to the applied pressure than the grain size as was also observed for medium or high SFE fcc metals [9].

4. Conclusions

1. The low SFE in Ag caused a high degree of dislocation dissociation that hindered their annihilation thereby resulting in a very large dislocation density after both ECAP- and HPT-processing.
2. The minimum grain size achieved by SPD in 4 N purity Ag was about 200 nm for both ECAP and HPT. However, the retarding effect of the high pressure in HPT on the dislocation annihilation resulted in a three times larger dislocation density than in ECAP-processing.
3. Due to the low SFE in Ag, twinning makes a significant contribution to plasticity during both ECAP and HPT. As twinning usually occurs at dislocation glide obstacles, therefore the higher dislocation density in the HPT-processed samples yield larger numbers of twin faults. The twin boundary frequency is also 2–3 times larger in the case of HPT, similar to the dislocation density.

Acknowledgements

This work was supported in part by the Hungarian Scientific Research Fund, OTKA, Grant No. K-81360, in part by the National Science Foundation of the United States under Grant No. DMR-0855009 (MK and TGL) and in part by the European Research Council under ERC Grant Agreement No. 267464-SPDMETALS (TGL). The European Union and the European Social Fund have provided financial support to this project under Grant Agreement No. TÁMOP 4.2.1./B-09/1/KMR-2010-0003. The authors thank Dr. Károly Havancsák, Gábor Varga and Andrea Jakab for taking the SEM images and preparation of the TEM samples.

References

[1] R.Z. Valiev, T.G. Langdon, Prog. Mater. Sci. 51 (2006) 881–981.
[2] A.P. Zhilyaev, T.G. Langdon, Prog. Mater. Sci. 53 (2008) 893–979.
[3] H. Jiang, Y.T. Zhu, D.P. Butt, I.V. Alexandrov, T.C. Lowe, Mater. Sci. Eng. A 290 (2000) 128–138.
[4] S.C. Baik, Y. Estrin, H.S. Kim, R. Hellmig, Mater. Sci. Eng. A 351 (2003) 86–97.
[5] E. Schafler, G. Steiner, E. Korznikova, M. Kerber, M.J. Zehetbauer, Mater. Sci. Eng. A 410–411 (2005) 169–173.
[6] E. Schafler, Scripta Mater. 62 (2010) 423–426.
[7] D. Setman, M.B. Kerber, E. Schafler, M.J. Zehetbauer, Metall. Mater. Trans. A 41 (2010) 810–815.
[8] J. Cizek, M. Janecek, O. Srba, R. Kuzel, Z. Barnovska, I. Prochazka, S. Dobatkin, Acta Mater. 59 (2011) 2322–2329.
[9] J. Gubicza, S.V. Dobatkin, E. Khosravi, A.A. Kuznetsov, J.L. Lábár, Mater. Sci. Eng. A 528 (2011) 1828–1832.
[10] S. Suwas, L.S. Tóth, J.-J. Fundenberger, W. Skrotzki, Scripta Mater. 49 (2003) 1203–1208.
[11] H. Matsunaga, Z. Horita, Mater. Trans. 50 (2009) 1633–1637.
[12] J. Gubicza, N.Q. Chinh, J.L. Lábár, Z. Hegedűs, T.G. Langdon, Mater. Sci. Eng. A. 527 (2010) 752–760.
[13] M. Furukawa, Y. Iwahashi, Z. Horita, M. Nemoto, T.G. Langdon, Mater. Sci. Eng. A 257 (1998) 328–332.
[14] Y. Iwahashi, J. Wang, Z. Horita, M. Nemoto, T.G. Langdon, Scripta Mater. 35 (1996) 143–146.
[15] G. Ribárik, J. Gubicza, T. Ungár, Mater. Sci. Eng. A 387-389 (2004) 343–347.
[16] R.B. Figueiredo, P.R. Cetlin, T.G. Langdon, Acta Mater. 55 (2007) 4769–4779.
[17] R.W. Baluffi, J. Nucl. Mater. 69-70 (1978) 240–263.